Prometabolites Hot Paper

Deutsche Ausgabe: DOI: 10.1002/ange.201503094
Internationale Ausgabe: DOI: 10.1002/anie.201503094

Prometabolites of 5-Diphospho-*myo*-inositol Pentakisphosphate**

*Igor Pavlovic, Divyeshsinh T. Thakor, Laurent Bigler, Miranda S. C. Wilson, Debabrata Laha, Gabriel Schaaf, Adolfo Saiardi, and Henning J. Jessen**

Abstract: *Diphospho-myo-inositol phosphates (PP-InsP$_y$) are an important class of cellular messengers. Thus far, no method for the transport of PP-InsP$_y$ into living cells is available. Owing to their high negative charge density, PP-InsP$_y$ will not cross the cell membrane. A strategy to circumvent this issue involves the generation of precursors in which the negative charges are masked with biolabile groups. A PP-InsP$_y$ prometabolite would require twelve to thirteen biolabile groups, which need to be cleaved by cellular enzymes to release the parent molecules. Such densely modified prometabolites of phosphate esters and anhydrides have never been reported to date. This study discloses the synthesis of such agents and an analysis of their metabolism in tissue homogenates by gel electrophoresis. The acetoxybenzyl-protected system is capable of releasing 5-PP-InsP$_5$ in mammalian cell/tissue homogenates within a few minutes and can be used to release 5-PP-InsP$_5$ inside cells. These molecules will serve as a platform for the development of fundamental tools required to study PP-InsP$_y$ physiology.*

Phosphorylated compounds, especially those derived from *myo*-inositol, play a pivotal role in cell signaling events. This signaling family comprises *myo*-inositol phosphates (InsP$_y$), diphospho-*myo*-inositol phosphates (X-PP-InsP$_y$, with X indicating the position of the diphosphate on the inositol scaffold), and the lipid-bound phosphatidyl-*myo*-inositol phosphates (PInsP$_y$).[1] Cell-permeable and photocaged analogues of InsP$_y$ and PInsP$_y$ have emerged as powerful compounds to study the functions of these molecules in cells.[2] Ideally, cell-permeable (nonpolar) prometabolites are stable outside cells but are converted by enzymes inside the cytoplasm (biolabile protection; for two examples, see Figure 1 B) to release the bioactive charged compound (highly polar). The absence of similar cell-permeable analogues of X-PP-InsP$_y$, such as **1** (Figure 1 A), motivated their design, synthesis, and evaluation.

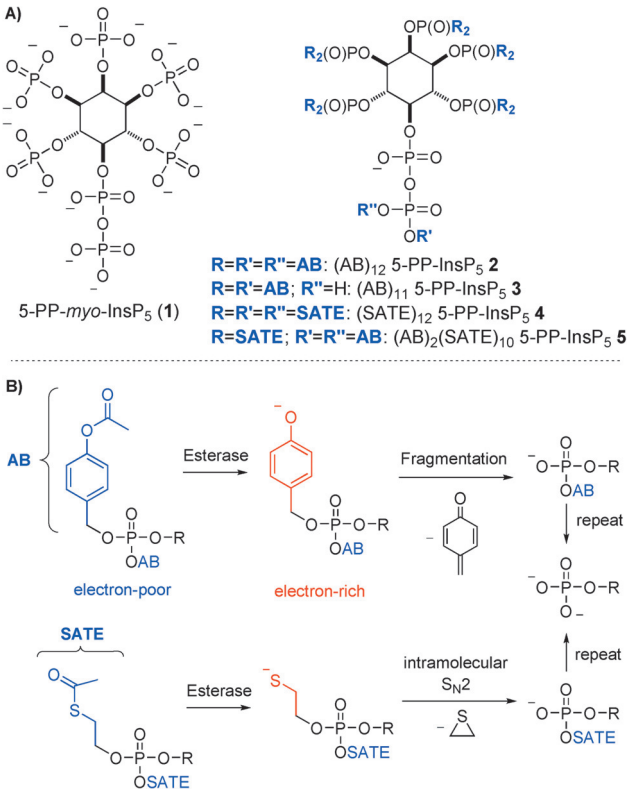

Figure 1. A) The most abundant mammalian diphosphoinositol phosphate 5-PP-InsP$_5$ (**1**) and several prodrugs (AB, SATE) targeted in this study (**2**–**5**). B) Cleavage of the different prodrug moieties (blue) is initiated by enzymatic hydrolysis of the ester groups, leading to unstable intermediates (red). These intermediates spontaneously release the parent phosphate. AB = acetoxybenzyl, SATE = *S*-acetylthioethyl.

The reason for the unavailability of cell-permeable analogues of X-PP-InsP$_y$ (for potential candidates, see Figure 1, compounds **2**–**5**) lies in the difficult preparation and design of prometabolites of phosphate anhydrides. Whereas various bioreversible protecting groups are available for phosphates,[3] thus far only one approach for phosphate anhydrides (P-anhydrides) has been successful.[4] However, this was achieved in a different context: Acyloxybenzyl[5] protection (Figure 1 B) led to antiviral prodrugs of nucleoside diphosphates.

In 5-PP-InsP$_5$ (**1**), the presence of one P-anhydride and five additional phosphate monoesters that require bioreversible protection complicates the synthesis and potentially the release efficacy. Overall, twelve to thirteen biolabile protecting groups need to be attached to the parent compound 5-PP-

[*] I. Pavlovic,[+] D. T. Thakor,[+] Priv.-Doz. Dr. L. Bigler, Prof. Dr. H. J. Jessen
Department of Chemistry, University of Zürich (UZH)
Winterthurerstrasse 190, 8057 Zürich (Switzerland)
E-mail: Henningjacob.jessen@chem.uzh.ch
Dr. M. S. C. Wilson, Prof. Dr. A. Saiardi
LMCB, University College London (UK)
D. Laha, Dr. G. Schaaf
Center for Plant Molecular Biology
University of Tübingen (Germany)
[+] These authors contributed equally to this work.

[**] This work was supported by the SNSF (PP00P2_157607 to H.J.J.), the MRC (MC_UU_1201814 to A.S.), and the DFG (Emmy Noether grant SCHA 1274/2-1 to G.S.).
Supporting information for this article is available on the WWW under http://dx.doi.org/10.1002/anie.201503094.

$InsP_5$ (**1**; Figure 1, **2**–**5**). With respect to its metabolism, additional unsolved problems arise from the challenging degradation studies that are required to verify the release of 5-PP-$InsP_5$ (**1**): As the product is highly polar and not UV-active, it cannot be detected by standard methods, such as HPLC analysis with UV detection.

Herein, evidence is provided that protection with twelve biolabile protecting (bp) groups of the P-esters and P-anhydrides on a highly congested *myo*-inositol scaffold is synthetically feasible. A modular synthesis is shown, which facilitates the introduction and combination of different bp groups (AB = acetoxybenzyl, SATE = *S*-acetylthioethyl; Figure 1 A,B). The degradation profile and the cellular uptake were furthermore analyzed by polyacrylamide gel electrophoresis (PAGE) in combination with TiO_2 based inositol phosphate extraction and mass spectrometry.[6]

The synthesis commenced with previously reported benzylidene acetal **6**,[7] which was phosphorylated with β-cyanoethyl P-amidite **7** in the 5-position (Scheme 1). After cleavage of the benzylidene acetal and the *para*-methoxybenzyl groups, phosphate triester **11** was phosphitylated with P-amidites **8**[4a] and **9**,[8] which contain bp groups, followed by oxidation to give hexakisphosphates **12** and **13**. These bp groups were chosen as they can be incorporated by P-amidite chemistry,[9] which leads to a flexible synthetic approach.[10]

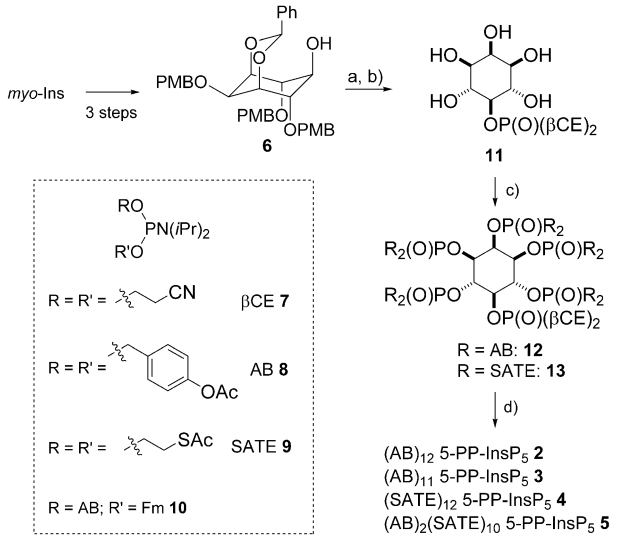

Scheme 1. Seven-step synthesis of the different prodrugs **2**–**5** starting from *myo*-inositol. The dotted box contains the P-amidites **7**–**10** used in this study. a) **7**, DCI, then *t*BuOOH; b) 5% TFA in DCM, 85 ± 4% (two steps); c) for **12**: **8**, DCI, then *m*CPBA, 47 ± 5%; for **13**: **9**, DCI, then *m*CPBA, 41%; d) for **2**: **12**, DBU, BSTFA, then MeOH, TFA, then **8**, tetrazole, then *m*CPBA, 73 ± 2%; for **3**: **12**, DBU, BSTFA, then MeOH, TFA, then **10**, tetrazole, then *m*CPBA, then piperidine, 46%; for **4**: **13**, DBU, BSTFA, then MeOH, TFA, then **9**, tetrazole, then *m*CPBA, 77%; for **5**: **13**, DBU, BSTFA, then MeOH, TFA, then **8**, tetrazole, then *m*CPBA, 75%. If possible, yields are given as averages of three independent experiments with standard deviation. Overall yield of **2** from **6**: approximately 29%. βCE = β-cyanoethyl, BSTFA = *N*,*O*-bis(trimethylsilyl)trifluoroacetamide, DCI = 4,5-dicyanoimidazole, Fm = fluorenylmethyl, Ins = inositol, *m*CPBA = *meta*-chloroperbenzoic acid, PMB = *para*-methoxybenzyl, TFA = trifluoroacetic acid.

The use of orthogonal protecting groups facilitated the generation of bioreversibly protected P-anhydrides in a one-pot process. This method has been developed for the generation of benzyl-protected X-PP-$InsP_5$[7,11] and 1/3,5-$(PP)_2$-$InsP_4$[12] and has additionally been applied in the synthesis of 5-PP-$InsP_4$.[13] Notably, the application of this method leaves the α-phosphate unprotected: The negative charge on this phosphate is required to obtain an inert, terminally protected P-anhydride that does not rapidly hydrolyze under aqueous conditions. Modification of the method allowed the introduction of both $(AB)_2$ and $(SATE)_2$ phosphates and the generation of a terminally monoprotected AB analogue as in **3**. This was achieved by the development of nonsymmetric P-amidite **10** containing both an AB and a fluorenylmethyl group, which can be removed selectively. Even though well-resolved ^{31}P NMR spectra of **3** could not be obtained, the identity and purity of the compound were verified by mass spectrometry and HPLC analysis, respectively (see the Supporting Information). Overall, mono-SATE-protected 5-PP-$InsP_5$ (**4**), a SATE analogue with a β-$(AB)_2$ P-anhydride (**5**), an $(AB)_2$-protected 5-PP-$InsP_5$ (**2**), and another $(AB)_2$ analogue with a β-AB P-anhydride (**3**) were synthesized.

Next, all compounds **2**–**5** were studied in different media to understand their metabolism (see the Supporting Information). The $(AB)_2$ protected analogue **2** was highly lipophilic and displayed only little solubility in aqueous buffers. Although precipitation complicated the analysis, it was possible to study the metabolism of **2** in tissue homogenates, as initial cleavage processes led to dissolution over time. The solubility of AB analogue **3** was superior to that of **2** owing to its two negative charges. The SATE-protected compounds **4** and **5** were both soluble in water (30 μM).

An important goal of this project was the identification of a compound that would be lipophilic but rapidly converted into highly polar 5-PP-$InsP_5$ (**1**) in cell/tissue homogenates. As the twelve bp groups in **2**–**5** would be cleaved sequentially and probably without regio- and chemoselectivity, many different intermediates were expected to be formed. Moreover, during the cleavage process, the intermediates become increasingly polar and less UV-active. The eventually released 5-PP-$InsP_5$ (**1**) has an estimated number of six to eight negative charges at physiological pH values and is not UV-active.[14]

To visualize the release process, a recently developed method for inositol phosphate analysis[6a–c] was applied to study the in vitro metabolism of inositol phosphate analogues (Figure 2). Briefly, in vitro reactions were resolved by PAGE, and bands were visualized by staining the gels with toluidine blue, a positively charged dye that binds to phosphates (Figure 2). The resolved bands were additionally extracted from the gels and analyzed by mass spectrometry (see the Supporting Information).

The different analogues **2**–**5** were incubated in freshly prepared brain and liver homogenates from rats and in freshly prepared cell (HCT116, MCF7, U2OS), yeast (*vtc4*Δ), plant (*Arabidopsis thaliana*), and *Dictyostelium discoideum* extracts, and the mixtures were directly loaded on gels (Figure 2, see also the Supporting Information). $(AB)_{12}$ analogue **2** was efficiently hydrolyzed to 5-PP-$InsP_5$ (**1**) in

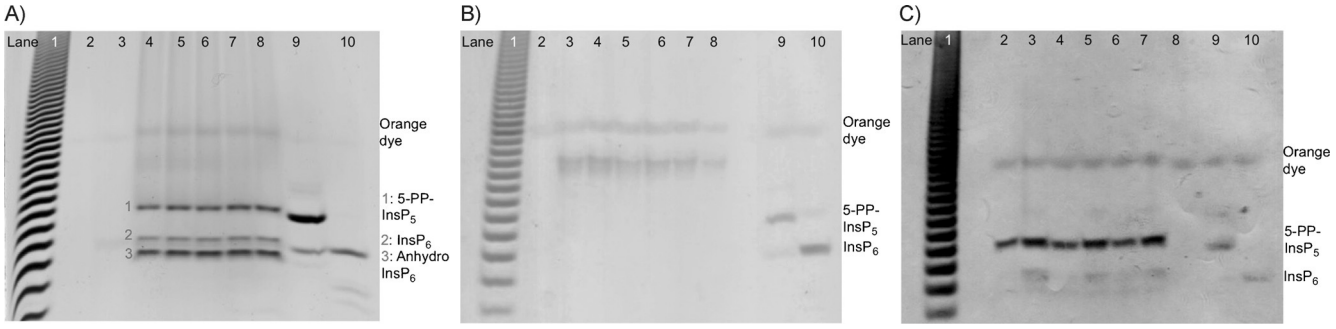

Figure 2. PAGE analysis of compounds **2**–**4** incubated in HCT116 cell extract. Orange G was used as the standard (horizontal) and polyP as the marker to assess the quality of separation (vertical). After resolution, gels were stained with toluidine blue. In the control lanes marked with *, the compounds migrated slightly faster owing to the absence of cell extract. In these lanes, Orange G also migrated faster. When controls were spiked into the samples (e.g., C, lanes 3, 5, and 7), comigration was observed. A) Time-dependent deprotection of **2** in HCT116 extract. After only 10 min, 5-PP-$InsP_5$ (**1**) was released with no further significant change at longer incubation times of up to three hours. In addition, $InsP_6$ was released and an unknown band 3 formed (see Figure 3 for the identification of the corresponding compound). Lane 1: polyP. Lane 2: **2** untreated (control). Lane 3: HCT116 cell extract (control). Lane 4: **2**/HCT116, 10 min. Lane 5: **2**/HCT116, 30 min. Lane 6: **2**/HCT116, 1 h. Lane 7: **2**/HCT116, 2 h. Lane 8: **2**/HCT116, 3 h. Lane 9: 5-PP-$InsP_5$ (**1**; control)*. Lane 10: $InsP_6$ (control)*. B) Time-dependent deprotection of **4** in a HCT116 extract. Only incomplete cleavage was observed in this experiment. Lane 1: polyP. Lane 2: **4** (control). Lane 3: **4**/HCT116, 4 h. Lane 4: **4**/HCT116, 3 h. Lane 5: **4**/HCT116, 2 h. Lane 6: **4**/HCT116, 1 h. Lane 7: **4**/HCT116, 30 min. Lane 8: **4**/HCT116, 10 min. Lane 9: 5-PP-$InsP_5$ (**1**; control)*. Lane 10: $InsP_6$ (control)*. C) Time-dependent deprotection of **3** in HCT116 extract. Cleavage was observed, and the side product formation was significantly reduced compared to A. Lane 1: polyP. Lane 2: **3**/HCT, 1 h. Lane 3: **3**/HCT, 1 h, spiked with additional $InsP_6$ (ca. 2 μg) and 5-PP-$InsP_5$ (ca. 2 μg). Lane 4: **3**/HCT, 30 min. Lane 5: **3**/HCT, 30 min, spiked with additional 5-PP-$InsP_5$ (ca. 2 μg). Lane 6: **3**/HCT, 10 min. Lane 7: **3**/HCT, 10 min, spiked with additional 5-PP-$InsP_5$ (ca. 2 μg). Lane 8: **3** (control). Lane 9: 5-PP-$InsP_5$ (**1**; control)*. Lane 10: $InsP_6$ (control)*.

all mammalian tissues and mammalian cell homogenates in as little as five minutes (Figure 2A, see also the Supporting Information). Despite the many possible side products, PAGE analysis reproducibly displayed only three defined bands (numbered in gel A). The *Dictyostelium* extract was capable of releasing 5-PP-$InsP_5$ (**1**), albeit at reduced rates (see the Supporting Information). We were unable to detect 5-PP-$InsP_5$ (**1**) release from **2** after incubation with yeast or plant extracts (see the Supporting Information). However, in contrast to yeast extracts, where no hydrolysis was observed, plant extracts efficiently hydrolyzed **2** to $InsP_6$, even in the presence of NaF, in a time-dependent manner (see the Supporting Information).

Whereas $(SATE)_{12}$ prometabolite **4** was more soluble than $(AB)_{12}$ **2**, incubation of **4** in different cell and tissue homogenates did not lead to release of 5-PP-$InsP_5$ (**1**) and only generated multiple bands on PAGE, which likely correspond to intermediates in which the SATE groups have been only partially removed (Figure 2B, see also the Supporting Information). To determine whether the SATE groups were only removed on the monophosphates but not on the phosphoanhydride, prometabolite **5** was analyzed, in which the P-anhydride is protected with two AB groups. Again, only incomplete cleavage, but not 5-PP-$InsP_5$ (**1**), was observed by PAGE (see the Supporting Information). This part of the study thus identified the AB system as superior to the SATE system, albeit at the cost of diminished aqueous solubility.

It was now important to understand how the three-band pattern was generated from $(AB)_{12}$ prometabolite **2** (Figure 2A). The first band comigrated with a 5-PP-$InsP_5$ (**1**) standard and the second band with an $InsP_6$ standard. The formation of both of these products was expected as, for example, diphosphoinositol phosphate phosphohydrolases (DIPPs) cleave the diphosphate in X-PP-$InsP_5$ to yield $InsP_6$.[15] The addition of NaF inhibits these phosphatases and indeed led to a slightly less intense $InsP_6$ band upon simultaneous treatment of **2** with brain homogenate and NaF (see the Supporting Information). However, $InsP_6$ was still detected and is likely the product of the chemical hydrolysis of the P-anhydride. In this context, it is very important that the $(AB)_{11}$ prometabolite **3**, which features an additional negative charge on the P-anhydride and is thus more stable towards chemical hydrolysis, showed only a very faint second band corresponding to $InsP_6$ (Figure 2C, see also the Supporting Information) and almost exclusively released 5-PP-$InsP_5$ (**1**) within a few minutes.

To further characterize the nature of the three products released from **2**, they were separated and isolated (Figure 3). A gel was run in which all lanes were loaded with the hydrolysis mixture of **2** in HCT cell extract. The gel was cut into pieces, according to the migration of the different bands, and the gel pieces were extracted.[6b] The extracted compounds were analyzed by mass spectrometry. The obtained MS spectra identified 5-PP-$InsP_5$ (**1**; band 1) and $InsP_6$ (band 2) despite polymeric debris from the extraction. The compound present in the third band had a mass peak corresponding to $InsP_6$ −18 mass units ($-H_2O$), and thus a cyclic anhydro structure **14** can be postulated (Figure 4). It is likely that this compound is formed in a non-enzymatic process: During cleavage of the AB groups, a nucleophilic attack of a (partially) deprotected phosphate adjacent to an intact $(AB)_2$-protected anhydride occurs, in which the good leaving group $(AB)_2$ phosphate is expelled. In contrast, the AB phosphate in **3** already harbors one additional negative charge and is consequently not such a good leaving group

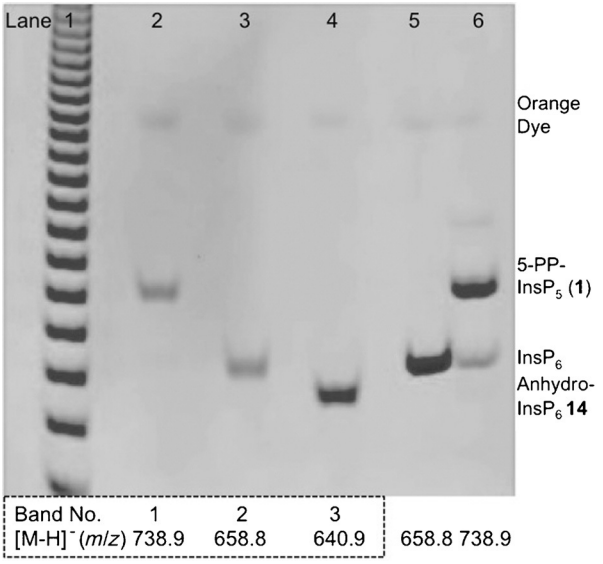

Figure 3. Separation of bands 1–3 after a preparative gel analysis as shown in Figure 2A. The bands were extracted and analyzed by MALDI mass spectrometry (the masses are shown underneath the gel). 5-PP-$InsP_5$ (**1**) and $InsP_6$ were clearly identified. Band 3 corresponds to $InsP_6$−18 mass units, and thus structure **14** was proposed. Lane 1: polyP marker. Lane 2: Band 1 from gel 2A (5-PP-$InsP_5$ **1**). Lane 3: Band 2 from gel 2A ($InsP_6$). Lane 4: Band 3 from gel 2A (anhydro-$InsP_6$ **14**). Lane 5: $InsP_6$ (standard). Lane 6: 5-PP-$InsP_5$ (**1**; standard).

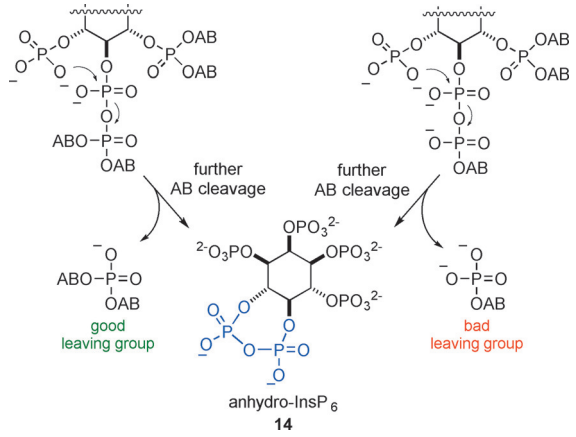

Figure 4. Cleavage mechanism for partially deprotected AB prodrugs. The $(AB)_2$-modified anhydride (left) is a good leaving group, promoting the formation of anhydro-$InsP_6$ (**14**). The AB-modified anhydride (right) is a poor leaving group. This mechanism explains the formation of anhydro-$InsP_6$ (**14**; Figure 2A) and also the reduced amount of **14** generated from **3** (Figure 2C) compared to that generated from prometabolite **2**.

(Figure 4). The increased chemical stability of a doubly charged P-anhydride thus explains the significant reduction of the amounts of both $InsP_6$ and anhydro-$InsP_6$ (**14**) released from prometabolite **3**. This result represents another significant finding as for studies of the function of 5-PP-$InsP_5$ (**1**) in cellulo, the generation of related side products, such as $InsP_6$ and anhydro-$InsP_6$ **14**, needs to be minimized (for a densitometric analysis, see the Supporting Information).

Next, the ability of both compounds **2** and **3** to cross the cell membrane and to release 5-PP-$InsP_5$ (**1**) in intact cells was studied. HCT116 cells were incubated with **2** and **3** for several hours. The cells were repeatedly washed and then lysed. PP-$InsP_y$ and $InsP_y$ (and other cellular phosphates) were subsequently enriched from the lysates using a novel TiO_2 nanoparticle extraction method to enable resolution and visualization by PAGE analysis (Figure 5, see also the

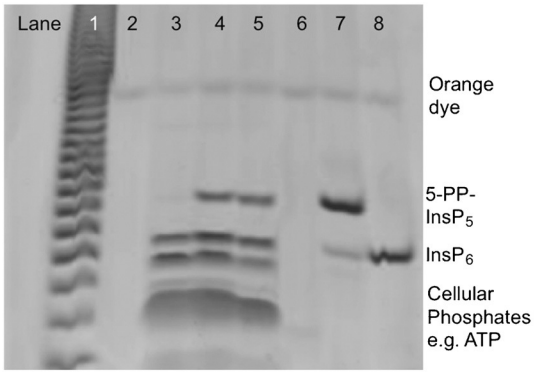

Figure 5. Cellular uptake and cleavage of **2** in HCT116 cells. HCT116 cells were incubated for multiple hours with **2**, then washed and lysed. Phosphate-containing molecules were enriched from the lysate by TiO_2 bead extraction and then loaded on the gel. Lane 1: polyP marker. Lane 2: **2** (control). Lane 3: HCT116 cells (control). Lane 4: HCT116/**2**, 24 h. Lane 5: HCT116/**2**, 48 h. Lane 6: ATP (control). Lane 7: 5-PP-$InsP_5$ (**1**; control). Lane 8: $InsP_6$ (control).

Supporting Information).[6d] Compound **2** showed robust release of 5-PP-$InsP_5$ (**1**) in cellulo, but owing the presence of multiple bands also in the control (Figure 5, lane 3), it could not be determined whether $InsP_6$ and anhydro-$InsP_6$ (**14**) were also released. Whereas **3** displayed almost exclusive release of 5-PP-$InsP_5$ (**1**) in vitro, cellular uptake was reduced compared to that of **2**, which is likely a consequence of the additional negative charge. However, this compound also released 5-PP-$InsP_5$ (**1**) in cellulo (see the Supporting Information).

In summary, the synthesis of highly congested prometabolites of 5-PP-$InsP_5$ (**2**–**5**) has been reported. Importantly, the AB system is generally suitable for the release of 5-PP-$InsP_5$ (**1**) in mammalian tissue and cell homogenates. Although robust hydrolysis of **2** was observed in extracts of slime mold and plants (but not in yeast extracts), future research will have to address whether the formation of small amounts (slime mold) or the absence (plant) of 5-PP-$InsP_5$ (**1**) in these reactions were caused by the instability of 5-PP-$InsP_5$ (**1**) in the respective extracts. The optimization of these approaches is also attractive for applications in plant cells, as recent results showcase the importance of X-PP-$InsP_y$ in the regulation of the wound responses in *Arabidopsis thaliana*.[16] By using PAGE analysis, different metabolites were assigned from mammalian tissue homogenates. Furthermore, by extracting the compounds from the gels, the previously unknown side product anhydro-$InsP_6$ (**14**) could be delineated. To suppress formation of **14**, a different AB analogue **3** with only one terminal biolabile protecting group

on the P-anhydride was developed. The hydrolysis profile obtained from compound **3** showed almost exclusive release of 5-PP-InsP_5 (**1**) in mammalian cell extracts. Significantly, both prometabolites **2** and **3** also released 5-PP-InsP_5 (**1**) in intact HCT116 cells. The AB system will now require further optimization to increase the solubility of the prometabolites and to improve cellular delivery. In the AB system, for example, the rate of hydrolysis could be fine-tuned by modulating the acyl moiety, and solubilizing groups could be attached to the aromatic portion. Finally, the prometabolites could be equipped with photocages to enable the modulation of the X-PP-InsP_5 concentration with temporal and spatial resolution inside living cells.

Keywords: Inositol pyrophosphates · metabolism · protecting groups · second messengers

How to cite: *Angew. Chem. Int. Ed.* **2015**, *54*, 9622–9626
Angew. Chem. **2015**, *127*, 9758–9762

[1] a) B. V. L. Potter, D. Lampe, *Angew. Chem. Int. Ed. Engl.* **1995**, *34*, 1933–1972; *Angew. Chem.* **1995**, *107*, 2085–2125; b) R. F. Irvine, M. J. Schell, *Nat. Rev. Mol. Cell Biol.* **2001**, *2*, 327–338; c) M. Bennett, S. M. N. Onnebo, C. Azevedo, A. Saiardi, *Cell. Mol. Life Sci.* **2006**, *63*, 552–564; d) M. J. Berridge, *Biochim. Biophys. Acta Mol. Cell. Res.* **2009**, *1793*, 933–940; e) S. B. Shears, *Mol. Pharmacol.* **2009**, *76*, 236–252; f) M. D. Best, H. L. Zhang, G. D. Prestwich, *Nat. Prod. Rep.* **2010**, *27*, 1403–1430; g) M. S. C. Wilson, T. M. Livermore, A. Saiardi, *Biochem. J.* **2013**, *452*, 369–379; h) M. P. Thomas, B. V. L. Potter, *FEBS J.* **2014**, *281*, 14–33.

[2] a) M. Vajanaphanich, C. Schultz, M. T. Rudolf, M. Wasserman, P. Enyedi, A. Craxton, S. B. Shears, R. Y. Tsien, K. E. Barrett, A. Traynor-Kaplan, *Nature* **1994**, *371*, 711–714; b) W. H. Li, C. Schultz, J. Llopis, R. Y. Tsien, *Tetrahedron* **1997**, *53*, 12017–12040; c) W. H. Li, J. Llopis, M. Whitney, G. Zlokarnik, R. Y. Tsien, *Nature* **1998**, *392*, 936–941; d) X. N. Yang, M. Rudolf, R. A. Carew, M. Yoshida, V. Nerreter, A. M. Riley, S. K. Chung, K. S. Bruzik, B. V. L. Potter, C. Schultz, S. B. Shears, *J. Biol. Chem.* **1999**, *274*, 18973–18980; e) C. Dinkel, M. Moody, A. Traynor-Kaplan, C. Schultz, *Angew. Chem. Int. Ed.* **2001**, *40*, 3004–3008; *Angew. Chem.* **2001**, *113*, 3093–3096; f) V. Laketa, S. Zarbakhsh, E. Morbier, D. Subramanian, C. Dinkel, J. Brumbaugh, P. Zimmermann, R. Pepperkok, C. Schultz, *Chem. Biol.* **2009**, *16*, 1190–1196; g) D. Subramanian, V. Laketa, R. Müller, C. Tischer, S. Zarbakhsh, R. Pepperkok, C. Schultz, *Nat. Chem. Biol.* **2010**, *6*, 324–326; h) M. Mentel, V. Laketa, D. Subramanian, H. Gillandt, C. Schultz, *Angew. Chem. Int. Ed.* **2011**, *50*, 3811–3814; *Angew. Chem.* **2011**, *123*, 3895–3898; i) M. P. Wymann, C. Schultz, *ChemBioChem* **2012**, *13*, 2022–2035; j) Y. Posor, M. Eichhorn-Gruenig, D. Puchkov, J. Schoneberg, A. Ullrich, A. Lampe, R. Muller, S. Zarbakhsh, F. Gulluni, E. Hirsch, M. Krauss, C. Schultz, J. Schmoranzer, F. Noe, V. Haucke, *Nature* **2013**, *499*, 233–237; k) D. Höglinger, A. Nadler, C. Schultz, *Biochim. Biophys. Acta Mol. Cell Biol. Lipids* **2014**, *1841*, 1085–1096; l) V. Laketa, S. Zarbakhsh, A. Traynor-Kaplan, A. Macnamara, D. Subramanian, M. Putyrski, R. Mueller, A. Nadler, M. Mentel, J. Saez-Rodriguez, R. Pepperkok, C. Schultz, *Sci. Signaling* **2014**, *7*, ra5.

[3] a) U. Pradere, E. C. Garnier-Amblard, S. J. Coats, F. Amblard, R. F. Schinazi, *Chem. Rev.* **2014**, *114*, 9154–9218; b) W. Chen, Z. Deng, K. Chen, D. Dou, F. Song, L. Li, Z. Xi, *Eur. J. Med. Chem.* **2015**, *93*, 172–181; c) A. J. Wiemer, D. F. Wiemer, *Top. Curr. Chem.* **2015**, *360*, 115–160.

[4] a) H. J. Jessen, T. Schulz, J. Balzarini, C. Meier, *Angew. Chem. Int. Ed.* **2008**, *47*, 8719–8722; *Angew. Chem.* **2008**, *120*, 8847–8850; b) F. Pertenbreiter, J. Balzarini, C. Meier, *ChemMedChem* **2015**, *10*, 94–106; c) T. Schulz, J. Balzarini, C. Meier, *ChemMedChem* **2014**, *9*, 762–775.

[5] W. Thomson, D. Nicholls, W. J. Irwin, J. S. Almushadani, S. Freeman, A. Karpas, J. Petrik, N. Mahmood, A. J. Hay, *J. Chem. Soc. Perkin Trans 1* **1993**, 1239–1245.

[6] a) O. Losito, Z. Szijgyarto, A. C. Resnick, A. Saiardi, *PLoS One* **2009**, *4*, e5580; b) O. Loss, C. Azevedo, Z. Szijgyarto, D. Bosch, A. Saiardi, *J. Visualized Exp.* **2011**, e3027; c) F. Pisani, T. Livermore, G. Rose, J. R. Chubb, M. Gaspari, A. Saiardi, *PLoS One* **2014**, *9*, e85533; d) M. S. C. Wilson, S. J. Bulley, F. Pisani, R. F. Irvine, A. Saiardi, *Open Biol.* **2015**, *5*, 150014.

[7] S. Capolicchio, D. T. Thakor, A. Linden, H. J. Jessen, *Angew. Chem. Int. Ed.* **2013**, *52*, 6912–6916; *Angew. Chem.* **2013**, *125*, 7050–7054.

[8] I. Lefebvre, C. Perigaud, A. Pompon, A. M. Aubertin, J. L. Girardet, A. Kirn, G. Gosselin, J. L. Imbach, *J. Med. Chem.* **1995**, *38*, 3941–3950.

[9] S. L. Beaucage, M. H. Caruthers, *Tetrahedron Lett.* **1981**, *22*, 1859–1862.

[10] a) G. S. Cremosnik, A. Hofer, H. J. Jessen, *Angew. Chem. Int. Ed.* **2014**, *53*, 286–289; *Angew. Chem.* **2014**, *126*, 290–294; b) H. J. Jessen, N. Ahmed, A. Hofer, *Org. Biomol. Chem.* **2014**, *12*, 3526–3530.

[11] M. X. Wu, L. S. Chong, S. Capolicchio, H. J. Jessen, A. C. Resnick, D. Fiedler, *Angew. Chem. Int. Ed.* **2014**, *53*, 7192–7197; *Angew. Chem.* **2014**, *126*, 7320–7325.

[12] S. Capolicchio, H. C. Wang, D. T. Thakor, S. B. Shears, H. J. Jessen, *Angew. Chem. Int. Ed.* **2014**, *53*, 9508–9511; *Angew. Chem.* **2014**, *126*, 9662–9665.

[13] H. C. Wang, H. Y. Godage, A. M. Riley, J. D. Weaver, S. B. Shears, B. V. L. Potter, *Chem. Biol.* **2014**, *21*, 689–699.

[14] C. E. Hand, J. F. Honek, *Bioorg. Med. Chem. Lett.* **2007**, *17*, 183–188.

[15] R. S. Kilari, J. D. Weaver, S. B. Shears, S. T. Safrany, *Febs Lett.* **2013**, *587*, 3464–3470.

[16] D. Laha, P. Johnen, C. Azevedo, M. Dynowski, M. Weiss, S. Capolicchio, H. Mao, T. Iven, M. Steenbergen, M. Freyer, P. Gaugler, M. K. F. de Campos, N. Zheng, I. Feussner, H. J. Jessen, S. C. M. Van Wees, A. Saiardi, G. Schaaf, *Plant Cell* **2015**, *27*, 1082–1097.

Received: April 3, 2015
Published online: May 26, 2015

